PHYSICAL REVIEW B **69**, 020401(R) (2004)

Heavy-fermion weak-ferromagnet YbRhSb

Y. Muro,[1] Y. Haizaki,[1] M. S. Kim,[1] K. Umeo,[1] H. Tou,[1] M. Sera,[1] and T. Takabatake[1,2]
[1]*Department of Quantum Matter, ADSM, Hiroshima University, Higashi-Hiroshima 739-8530, Japan*
[2]*Materials Science Center, N-BARD, Hiroshima University, Higashi-Hiroshima 739-8530, Japan*
(Received 25 August 2003; published 5 January 2004)

A new Yb-based compound YbRhSb with the orthorhombic ε-TiNiSi-type structure has been synthesized. The magnetic-susceptibility, magnetization, and specific-heat (C_p) measurements of single crystals revealed a ferromagnetic transition at $T_C = 2.7$ K. An extrapolation of the C_p/T data below 1 K yields 370 mJ/mol K^2 as the γ value, and the magnetic entropy reaches only $0.25R \ln 2$ at T_C. The spontaneous moment is unusually small, $3\times10^{-3}\mu_B$/Yb for $B||b$, while the magnetization increases to $1.4\mu_B$/Yb when the field of 15 T is applied along the *a* axis. We ascribe the weak ferromagnetism to a canted antiferromagnetic structure based on the observation of a metamagnetic transition and the decrease of T_C with the increase of magnetic field.

DOI: 10.1103/PhysRevB.69.020401 PACS number(s): 75.30.Mb, 75.20.Hr, 71.27.+a

Heavy-fermion (HF) compounds have attracted considerable attention because of the appearance of unconventional superconductivity and non-Fermi-liquid behaviors in the vicinity of a boundary between the magnetically ordered state and the paramagnetic state, so-called a quantum critical point (QCP).[1] Interestingly, ferromagnetic HF compounds are rather rare compared with antiferromagnetic HF compounds. Recently, weak ferromagnetism (WFM) has been found in $Yb_{1-x}Y_xInCu_4$ ($x \leqslant 0.3$) under pressure,[2–4] and coexistence of ferromagnetism with unconventional superconductivity has been observed in UGe_2 and URhGe.[5,6] Although the fundamental mechanisms remain unknown, these findings have caused great interest in ferromagnetic HF compounds.

YbNiSn also exhibits unusual ferromagnetic properties.[7–9] This compound crystallizes in the orthorhombic ε-TiNiSi-type structure. The isostructural Ce-based counterpart CeNiSn is well known as a Kondo semiconductor.[10] YbNiSn undergoes a ferromagnetic transition at $T_C = 5.6$ K with the ordered moment $M_s = 0.85\mu_B$.[7] A large electronic specific-heat coefficient ($\gamma \simeq 300$ mJ/mol K^2) below T_C classified YbNiSn into the HF system.[8] A neutron-diffraction study revealed the collinear magnetic structure with magnetic moments along the *c* axis although the easy magnetization axis is *a* axis.[7] An unusual pressure dependence of T_C was found;[9] T_C increases to 7.6 K on applying pressure up to 2 GPa while the magnitude of M_s is unchanged, and a complex antiferromagnetic order appears at 3 GPa. These properties were explained by considering the volume-dependent competition between the anisotropy of the intersite exchange interaction and that due to the crystalline electric-field (CEF) effect. If the volume of YbNiSn could be expanded, the magnetically ordered state is destabilized and the system would be tuned toward the QCP. With this in mind, we have synthesized such an isostructural compound YbRhSb, the unit-cell volume of which is larger by 4% than that of the sister compound YbNiSn. In this paper, we report the magnetic, transport, and thermal properties of single-crystalline samples. The results of measurements revealed a WFM transition which occurs in a HF state. We discuss the origin of the WFM in YbRhSb by comparing the physical properties with those in YbNiSn.

Single-crystalline samples of YbRhSb were grown by using the Bridgeman method. Stoichiometric amounts of the elements were sealed in a molybdenum crucible by arc welding under a purified argon atmosphere. The crucible was heated up to 1600 °C in a vacuum by using a tungsten mesh heater and slowly cooled. The least-squares refinement of the powder x-ray-diffraction pattern showed that YbRhSb crystallizes with the orthorhombic ε-TiNiSi-type structure (space group *Pnma*) with lattice constants $a = 7.004$ Å, $b = 4.492$ Å, and $c = 7.731$ Å. Metallographic examination together with the electron-probe microanalysis (EPMA) revealed the presence of an impurity phase $YbSb_2$ of less than 0.1% of the stoichiometric host phase. The single-crystal nature of the sample was confirmed by the x-ray Laue diffraction method. The electrical resistivity was measured by the conventional dc four-probe method in the temperature range from 0.35 K to 300 K. The measurements of specific heat were performed by using the quasiadiabatic heat-pulse method between 0.6 K and 70 K in zero field and by the Physical Property Measurement System (Quantum Design) in magnetic field up to 10 T. Magnetization was measured by using a commercial superconducting quantum interference device magnetometer (Quantum Design) in fields up to 5 T at temperatures from 2 K to 300 K, and by a homemade extraction-type magnetometer for fields up to 15 T and temperatures down to 1.4 K.

Figure 1(a) shows the inverse magnetic susceptibility $\chi(T)^{-1}$ of YbRhSb for field directions parallel to the orthorhombic principal axes. The three sets of data of $\chi(T)$ from 300 K to 100 K obey the Curie-Weiss law with an effective magnetic moment μ_{eff} of $4.4\mu_B$ which is close to $4.54\mu_B$ expected for the free Yb^{3+} ion. The strong deviation from the Curie-Weiss law on cooling below 100 K can be ascribed to the CEF effect. The paramagnetic Curie temperatures (θ_p) are -47, -90, and -160 K for $B||a$, $B||b$, and $B||c$, respectively. The $\chi(T)$ for $B||a$ is the largest in the whole measured temperature range. This anisotropic behavior indicates that the magnetization easy axis in the paramagnetic state is parallel to the *a* axis, same as for YbNiSn.[8]

The anisotropic behavior in the electrical resistivity ρ is shown in Fig. 1(b). In a wide temperature range from 300 K to 50 K, $\rho(T)$ for all the current directions remains almost

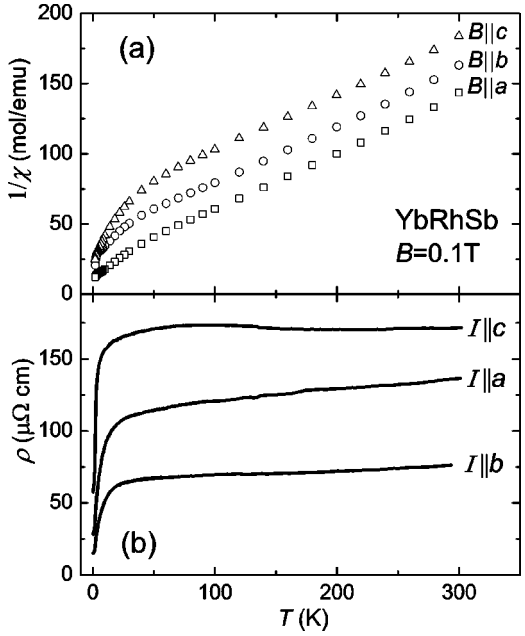

FIG. 1. Temperature dependence of (a) the magnetic susceptibility and (b) the electrical resistivity of single crystal YbRhSb for the directions of magnetic field and electrical current, respectively, along the orthorhombic crystal axes.

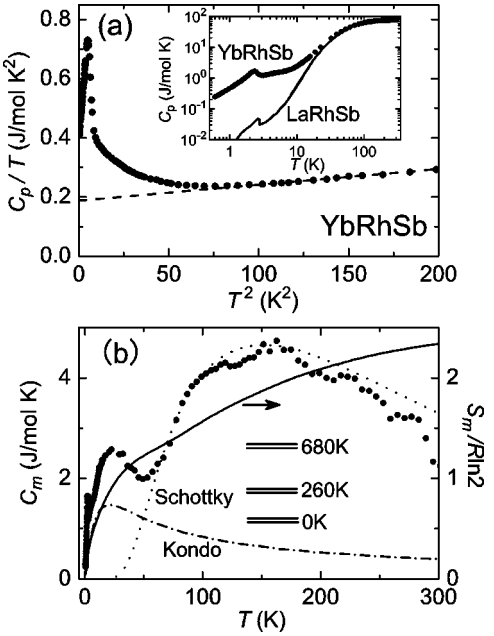

FIG. 2. (a) Temperature dependence of the specific heat C_p of YbRhSb plotted as C_p/T vs T^2. The dashed line represents the linear extrapolation to $T=0$ K. The inset shows the double-logarithmic plot of C_p vs T for YbRhSb and LaRhSb. (b) The magnetic part of specific heat C_m and magnetic entropy S_m divided by $R\ln 2$, where R is the gas constant. The dash-dotted line represents the theoretical curve of C_m for $S=1/2$ Kondo impurities with $T_K=30$ K, and the dotted line is the crystal-field contributions to C_m calculated using the energy scheme drawn in the inset.

constant, but rapidly decreases with decreasing temperature below 20 K. This behavior in $\rho(T)$ is common to Yb-based HF compounds such as YbNiSn and $YbRh_2Si_2$.[7,11] The low-temperature data of $\rho(T)$ will be shown and discussed afterward.

Figure 2 shows the result of the specific heat $C_p(T)$ of YbRhSb. As shown in Fig. 2(a), a linear extrapolation of the C_p/T vs T^2 plot from above 10 K yields the electronic specific-heat coefficient γ_H and the Debye temperature Θ_D to be 188 mJ/mol K^2 and 222 K, respectively. This magnitude of γ_H is transferred to the Kondo temperature T_K of 30 K by using the $S=1/2$ impurity Kondo model, which is relevant to a ground-state doublet of Yb^{3+}.[12] On cooling below 8 K, C_p/T increases significantly and exhibits a pronounced maximum at 2.7 K, which is due to a magnetic transition as is shown below. The magnetic contribution to the specific heat $C_m(T)$ was derived by the subtraction of C_p of LaRhSb from that of YbRhSb without any correction for the difference in the mass between La and Yb atoms. It should be noted that the anomaly in $C_p(T)$ for LaRhSb at 2.2 K is due to the superconducting transition.[13] The data of $C_m(T)$ displays two peaks at 25 K and 160 K, respectively. The former temperature agrees with the above-mentioned value of $T_K=30$ K, and the latter peak could be reproduced by the sum of Schottky peaks due to the CEF effect. In YbRhSb with the orthorhombic crystal symmetry, the CEF splits the eightfold degenerate $J=7/2$ state of Yb^{3+} ion into four doublets. For fitting Schottky anomalies, we neglected the contribution from the highest doublet because the magnetic entropy $S_m(T)$ seems to reach a value of $R\ln 6$ far above 300 K. The proposed level scheme is represented in Fig. 2(b). The fact that energy splitting between the ground-state doublet and the first exited doublet is twice that of YbNiSn ($\sim$150 K) is opposite to the expectation from the larger unit-cell volume by 4% for YbRhSb.[7] The S_m reaches $0.25R\ln 2$ at the magnetic ordering temperature, and this small value suggests the strong suppression of the magnetic entropy by the Kondo effect. With increasing temperature, S_m recovers the full value of $R\ln 2$ at 30 K which agrees with the T_K estimated from the γ_H value.

The magnetic transition at 2.7 K is manifested as anomalies in both M/B and ρ, as seen in Fig. 3. For all the principal directions, the data of M/B at $B=10$ mT turn upward below 3 K, where this temperature agrees with the λ-type anomaly in C_p/T [see Fig. 3(c)]. The drop of $\rho(T)$ is most pronounced for the current direction $I||c$. These findings indicate that a long-ranged magnetic transition takes place at $T_C=2.7$ K with a ferromagnetic component. As shown in the inset of Fig. 3(c), the linear extrapolation of the C_p/T vs T^2 plot below 1 K yields the γ_L value of 370 mJ/mol K^2. The transition is totally suppressed when the magnetic field of 10 T is applied along the a axis. More detailed analysis of $C_p(T)$ in magnetic fields will be reported elsewhere. The ferromagnetic nature was confirmed by the measurement of isothermal magnetization $M(B)$. In Fig. 4(a), a small but clear hysteresis loop is observed at 2 K in all principal directions. The spontaneous magnetization M_s is estimated by the linear extrapolation of the $M(B)$ data to $B=0$ to be $0.0018\mu_B$/Yb, $0.0032\mu_B$/Yb, and $0.0013\mu_B$/Yb for $B||a$, $B||b$, and $B||c$, respectively. It is noteworthy that $M_s(B||a)$, along the easy magnetization axis in the paramagnetic state,

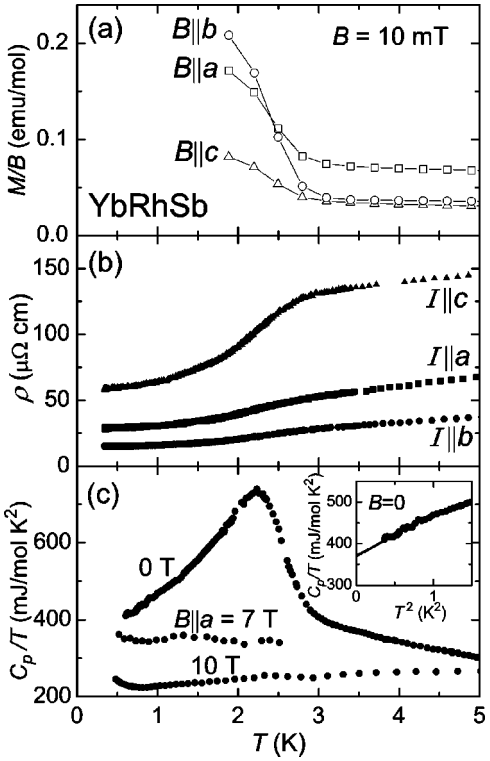

FIG. 3. (a) Low-temperature data of magnetic susceptibility M/B at $B=10$ mT, (b) electrical resistivity, and (c) specific heat in $B||a=0$, 7, and 10 T for YbRhSb. The inset represents the data plotted by C_p/T vs T^2.

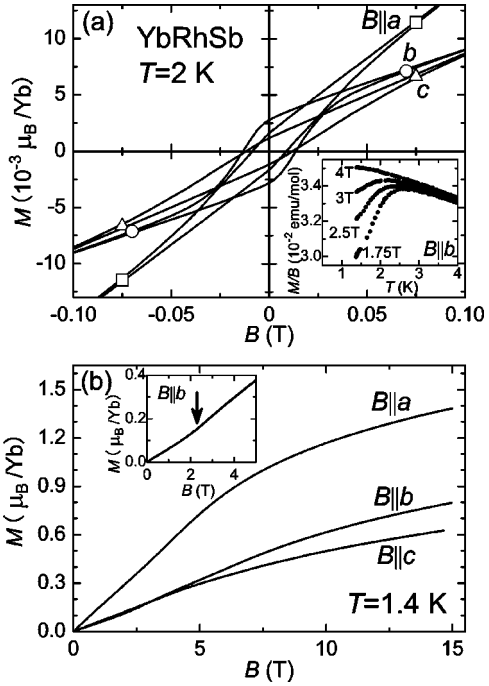

FIG. 4. (a) Isothermal magnetization curves $M(B)$ of YbRhSb at 2 K in the field range $|B|<0.1$ T. The inset shows the temperature dependence of the susceptibility M/B under various magnetic fields. (b) $M(B)$ curves at 1.4 K. The metamagnetic transition at 2.2 T for $B||b$ is shown in the inset.

is approximately half $M_s(B||b)$. In any events, the values of M_s are three orders of magnitude smaller than that expected for the CEF ground state of Yb^{3+}.

From the magnitude of $M_s \approx 10^{-3}\mu_B$/Yb, one would suspect that the WFM results from a small amount of ferromagnetic impurity. However, this can be ruled out by following reasons. First, among four single-crystal samples taken from different batches, no sample dependence was observed in either T_C or M_s along all the directions. Second, the impurity $YbSb_2$, whose volume fraction is less than 0.1% according to the EPMA, has been known as a Pauli paramagnet showing a superconducting transition at 1.4 K.[14] Thus, the WFM must be the intrinsic property of YbRhSb.

Figure 4(b) shows the $M(B)$ curves up to 15 T at 1.4 K. The $M(B)$ for $B||a$ and $B||c$ increases smoothly, and then reaches $1.4\mu_B$/Yb and $0.6\mu_B$/Yb, respectively, at the highest field. On the other hand, $M(B||b)$ exhibits a metamagneticlike anomaly at 2.2 T as shown more clearly in the inset of Fig. 4(b). Under various magnetic fields above and below 2.2 T, we measured the temperature dependence of $M(B||b)$ and the result of M/B vs T is represented in the inset of Fig. 4(a). The upturn in M/B at $B=10$ mT (see Fig. 3) changes to a peak at 2.4 K for $B=1.75$ T. The peak temperature decreases with increasing B up to 4 T. The decrease of the ordering temperature and the metamagneticlike anomaly are characteristic of an antiferromagnet rather than a ferromagnet. Therefore, the WFM moment in YbRhSb is not induced by a collinear ferromagnetic structure as found in the isostructural compound YbNiSn, but originated from a canted antiferromagnetic structure.

Now we consider the mechanism of WFM in YbRhSb. The occurrence of WFM in antiferromagnets may originate from two relevant interactions:[15] one is single-ion anisotropy due to the CEF and the other is the antisymmetric interaction, so-called Dzyaloshinsky-Moriya (DM) interaction induced by an anisotropic spin-spin interaction. First, we examine the possibility of the DM interaction for the WFM of YbRhSb. The nearest-neighbor Yb ions are placed in one *ac* plane and form a zigzag chain along the *a* axis. No inversion symmetry exists at the midpoint of two neighboring Yb ions, but the two Yb ions are in a mirror plane parallel to the *ac* plane. The mirror symmetry allows the Dzyaloshinsky vector at the midpoint to orient perpendicular to the *ac* plane.[15] Thus a ferromagnetic component can appear when the antiferromagnetic moments lie in the *ac* plane. However, the M_s of YbRhSb is the largest for $B||b$, and M/B decreases most significantly for $B||b$ on cooling below the peak temperature. These facts indicate that the ordered moments lie almost parallel to the *b* axis, which contradicts the above-mentioned requisite for the DM interaction. In order to confirm this reasoning, neutron-diffraction measurements have been performed on a single crystal above and below the ordering temperature. Preliminary results are consistent with the canted antiferromagnetic structure above proposed.[16]

In Yb-based compounds, single-ion anisotropy originates from the CEF-induced magnetocrystalline anisotropy, which determines the direction of the easy magnetization in the paramagnetic state. The easy magnetization direction agrees with the direction of the ordered moments if the magneto-

crystalline anisotropy due to the magnetic exchange interaction is sufficiently weak. In YbRhSb, the metamagnetic transition at 2.2 T for $B||b$ suggests the strong magnetocrystalline anisotropy. Moreover, the magnetization easy axis along the *a* axis is different from the direction of ordered moments which is almost along the *b* axis. As mentioned above, in the isostructural compound YbNiSn, the magnetization easy axis is the *a* axis while the ordered moments are directed to the *c* axis. It was ascribed to the competitive anisotropies between the CEF effect and the magnetic exchange interaction.[7] Furthermore, the pressure study of YbNiSn revealed that the volume dependence of the balance between the two anisotropies induces a complex antiferromagnetic state above 3 GPa.[9] The unit-cell volume of YbRhSb ($V=242.3$ Å^3) is larger by 4% than that of YbNiSn ($V=233.5$ Å^3) at room temperature. This size of volume expansion might be sufficient to quench the collinear ferromagnetic order because its T_C is expected to vanish at $V \sim 240$ Å^3 from the Grüneisen parameter $-d\ln T_C/d\ln V = -40$.[17] The instability of the collinear ferromagnetic state may favor the antiferromagnetic ground state. The delicate competition between the CEF effect and the magnetic exchange interaction may allow a canted antiferromagnetic structure in YbRhSb.

In summary, we have synthesized a new Yb-based compound YbRhSb with the ε-TiNiSi-type structure in a single-crystal form, and investigated the magnetic and transport properties. The magnetic susceptibility is governed by the combination of the CEF effect and Kondo effect. The electrical resistivity is characterized with a plateau down to 50 K and a rapid decrease on cooling below 20 K. A pronounced Kondo peak emerges in the magnetic contribution to the specific heat, which is reproduced by the Kondo impurity model with $T_K=30$ K. The most significant observation of this study is a ferromagnetic transition at $T_C=2.7$ K. An extrapolation of the C_p/T data below 1 K yields 370 mJ/mol K^2 as the γ value, and the magnetic entropy reaches only $0.25R\ln 2$ at T_C. The spontaneous magnetization at 2 K is largest for the field direction parallel to the *b* axis, while the *a* axis is the magnetization easy axis. Surprisingly enough, the magnitude of the spontaneous magnetization is only $0.0032\mu_B$/Yb that is smaller by three orders of magnitude than $4\mu_B$ that expected for a Yb^{3+} free ion. However, the magnetic moment increases to $1.4\mu_B$/Yb when the external field of 15 T is applied along the *a* axis. We therefore ascribe the WFM of YbRhSb to the result of a canted antiferromagnetic order. In fact, the antiferromagnetic nature is manifested in both the decrease of the peak temperature of the M/B vs T plot and the appearance of the metamagnetic transition at 2.2 T for $B||b$. To our knowledge, YbRhSb is the first example of Yb-based HF compound showing very small spontaneous moment at ambient pressure. Our considerations of the local symmetry of Yb^{3+} ions and of the volume dependence of the magnetic structure for the isostructural ferromagnet YbNiSn led us to conclude that the WFM of YbRhSb originates in the competition between the anisotropy due to CEF effect and that of the magnetic exchange interaction. In order to determine the magnetic structure and the size of the ordered moment, neutron-diffraction and NMR experiments are presently under way.

The authors are very grateful to Y. Shibata for the electron-probe microanalysis. We thank S. Nagai and K. Hirota for discussing their results of neutron-diffraction study. This work was supported by a Grant-in Aid for Scientific Research (COE Research under Grant No. 13CE2002) of MEXT Japan.

[1] For a review, see, e.g., G.R. Stewart, Rev. Mod. Phys. **73**, 797 (2001).

[2] A. Mitsuda, T. Goto, K. Yoshimura, W. Zhang, N. Sato, K. Kosuge, and H. Wada, Phys. Rev. Lett. **88**, 137204 (2002).

[3] N.V. Mushnikov, T. Goto, E.V. Rozenfeld, K. Yoshimura, W. Zhang, M. Yamada, and H. Kageyama, J. Phys.: Condens. Matter **15**, 2811 (2003).

[4] T. Mito, T. Koyama, M. Shimoide, S. Wada, T. Muramatsu, T.C. Kobayashi, and J.L. Sarrao, Phys. Rev. B **67**, 224409 (2003).

[5] S.S. Saxena, P. Agarwal, K. Ahilan, F.M. Grosche, R.K.W. Haselwimmer, M.J. Steiner, E. Pugh, I.R. Walker, S.R. Jullan, P. Monthoux, G.G. Lonzarich, A. Huxley, I. Sheikin, D. Braithwaite, and J. Flouquet, Nature (London) **406**, 587 (2000).

[6] D. Aoki, A. Huxley, E. Ressouche, D. Braithwaite, J. Flouquet, J. P. Brison, E. Lhotel, and C. Paulsen, Nature (London) **413**, 613 (2001).

[7] P. Bonville, P. Bellot, J.A. Hodges, P. Imbert, G. Jéhanno, G. Le Bras, J. Hammann, L. Leylekian, G. Chevrier, P. Thuéry, L. D'Onofrio, A. Hamzic, and A. Barthélémy, Physica B **182**, 105 (1992).

[8] M. Kasaya, T. Tani, K. Kawate, T. Mizushima, Y. Isikawa, and K. Sato, J. Phys. Soc. Jpn. **60**, 3145 (1991).

[9] K. Drescher, M.M. Abd-Elmeguid, H. Micklitz, and J.P. Sanchez, Phys. Rev. Lett. **77**, 3228 (1996).

[10] T. Takabatake, F. Teshima, H. Fujii, S. Nishigori, T. Suzuki, T. Fujita, Y. Yamaguchi, J. Sakurai, and D. Jaccard, Phys. Rev. B **41**, 9607 (1990).

[11] O. Trovarelli, C. Geibel, and F. Steglich, Physica B **284-288**, 1507 (2000).

[12] A.C. Hewson, *The Kondo Problem to Heavy Fermions* (Cambridge University Press, London, 1993).

[13] S.K. Malik, H. Takeya, and K.A. Gschneidner, Jr., Phys. Rev. B **48**, 9858 (1993).

[14] Y. Yamaguchi, S. Waki, and K. Mitsugi, J. Phys. Soc. Jpn. **56**, 419 (1987).

[15] T. Moriya, in *Magnetism I*, edited by G.T. Rado and H. Suhl (Academic, New York, 1963), p. 85.

[16] S. Nagai, K. Hirota, Y. Muro, Y. Haizaki, and T. Takabatake (unpublished).

[17] K. Drescher, M.M. Abd-Elmeguid, J.P. Sanchez, and C. Meyer, J. Phys.: Condens. Matter **8**, L65 (1996).